ELSEVIER

Palaeogeography, Palaeoclimatology, Palaeoecology 197 (2003) 113–131

PALAEO

www.elsevier.com/locate/palaeo

500 000-Year records of carbonate, organic carbon, and foraminiferal sea-surface temperature from the southeastern South China Sea (near Palawan Island)

Min-Te Chen [a,*], Liang-Jian Shiau [a], Pai-Sen Yu [a], Tzu-Chien Chiu [b], Yue-Gau Chen [b], Kuo-Yen Wei [b]

[a] *Institute of Applied Geophysics, National Taiwan Ocean University, Keelung 20224, Taiwan R.O.C.*
[b] *Department of Geosciences, National Taiwan University, Taipei, Taiwan R.O.C.*

Received 22 August 2001; received in revised form 29 April 2002; accepted 1 February 2003

Abstract

High-resolution records of planktic foraminifer sea-surface temperature (SST) and biogenic sediment components of carbonate and total organic carbon (TOC) concentrations were determined in an IMAGES giant piston core spanning ~the last 500 000 years, taken near the western slope of Palawan Island in the southeastern South China Sea (SCS). The records provide information of paleoceanographic and paleoclimatological variations linked to East Asian monsoon systems in the SCS, the largest marginal sea of the western Pacific. Constrained by planktic foraminifer (*Globigerinoides ruber*) oxygen isotope stratigraphies, the records show a lowering of faunal SST by ~3°C during glacial stages, indicating significant cooling in the glacial western Pacific climate. In general, they show low-frequency patterns with high SSTs, high carbonate content, and low TOC content during interglacial periods, and exhibit low SSTs, low carbonate content, and high TOC content during glacial periods. The carbonate content variations indicate that the sediment composition is mostly controlled by terrigenous inputs, which are associated with sea-level fluctuations in the SCS during past glacial–interglacial stages. The low SST and high TOC content indicate cooling and high productivity conditions in the surface oceans of the SCS, which also reflect a condition of intensified winter monsoon winds associated with glacial boundary conditions. Some rapid, high-frequency oscillations of the SST and TOC found in the records are coincident with intervals of intensified winter or summer monsoons from the Arabian Sea, implying that the Asian monsoon systems had wider regional effects than previously assumed. Time-series analyses reveal that variations in the SST, carbonate and TOC contents of this record contain statistically significant concentrations of variance at orbital frequency bands, namely 100 kyr^{-1}, 41 kyr^{-1}, and 23 kyr^{-1}, suggesting that both ice volume and orbital solar insolation changes are potential mechanisms for the SCS monsoon variations.

Keywords: planktic foraminifer; East Asian monsoon; South China Sea

1. Introduction

The strong winds associated with East Asian

* Corresponding author. Tel.: +886-2-2462-2192 x6503; Fax: +886-2-2462-5038.
E-mail address: mtchen@mail.ntou.edu.tw (M.-T. Chen).

0031-0182/03/$ – see front matter © 2003 Elsevier Science B.V. All rights reserved.
doi:10.1016/S0031-0182(03)00389-4

monsoons play an important role in governing seasonal patterns in the surface ocean hydrographies of the South China Sea (SCS). The monsoon, driven by the atmospheric pressure difference between land and ocean, generates seasonally reversible current systems in response to prevailing wind direction (Shaw and Chao, 1994). During the winter months (November–April), northeasterly winds bring cold air from the East Asian continent as well as from Chinese coastal water into the SCS through the Taiwan Straits, leading to the development of strong latitudinal gradients in sea-surface temperature (SST). This system is replaced during the summer months (May–October) by southwesterly winds, which bring an influx of warm and humid surface air. Warm Indian Ocean surface water also flows northward over the Sunda Shelf into the southern SCS. The summer season SSTs are high (~28°C) with relatively insignificant spatial variation. Observational and modeling studies indicate that the prevailing monsoon wind-induced Ekman pumping in the surface oceans results in winter upwelling off the northwestern Philippines (Shaw et al., 1996) and in summer upwelling along the eastern Vietnam margins (Wiesner et al., 1996; Ho et al., 2000).

Paleoceanographic investigations using deep-sea records of the past few glacial–interglacial cycles suggest that surface ocean temperature variability in the SCS is either dominated by monsoon wind processes (Huang et al., 1997a,b; Chen and Huang, 1998; Wang et al., 1999a,b; Chen et al., 1999) or largely controlled by sea-level fluctuations (Wang and Wang, 1990; Wang et al., 1995; Pelejero et al., 1999a,b). During the last glacial maximum (LGM), relatively cold surface temperatures over the East Asian continent and relatively warm western Pacific Ocean temperatures may have driven strong northeasterly winds, which in turn induced strong mixing and probably high productivity in the surface ocean of the SCS. The strong winds may have deepened the mixed-layer depth, and also carried large amounts of dust that may have been incorporated into biogenic particle aggregates, thereby increasing the transfer rate of organic matter from the surface to the deep sea (Ittekkot et al., 1992). The transfer rate may have been even higher, since large quantities of riverine nutrients and mineral particles are laterally advected to the SCS from large rivers such as the Changjiang (Yangtze River) and Zhunjiang (Pearl River) (Ittekkot et al., 1991; Wiesner et al., 1996). On the other hand, lowering sea-levels gave rise to an emerged continental shelf around the SCS, and consequently restricted the inflow of warm waters from the open oceans. For example, the emergent Sunda Shelf in the southern part of the SCS may have precluded any exchange with tropical Indian and Pacific surface waters. These reduced inflows may have led to decreased SSTs in the SCS. Under glacial low sea-level conditions, the depocenter may have shifted toward the outer shelf and continental slope (Schonfeld and Kudrass, 1993). This process may have brought more suspended fine-grained fluvial terrigenous sediments to the slope with an increased accumulation rate, a condition favorable for enhanced organic matter preservation in marine sediments (Müller and Suess, 1979; Sarnthein et al., 1988).

Previous SCS paleoceanographic studies concentrated on the past glacial–interglacial variations. There is a lack of long records (~500 000 years) from the SCS to constrain the past variations at orbital time scales. Moreover, there is also a lack of comparisons on paleomonsoon records of the SCS and of the Arabian Sea, Indian Ocean. To this end, here we examined variations in planktic foraminifer faunal assemblages and stable isotopes, as well as biogenic carbonate and organic carbon concentrations (wt%) and mass accumulation rates (MARs) based on an IMAGES (International Marine Global Change Study) core (MD972142) from the southeastern SCS near Palawan Island (Fig. 1). The modern SST at the coring site is ~28°C and the seasonal variation of the SST is minimal (NOAA, 1994). This site is located far away from the large rivers that drain into the SCS. Biogenic sediment preservation resulting from lateral advection of riverine material supply is thought to be minimal in the SCS, therefore the core taken from this area is ideal for examining past surface ocean variability associated with East Asian monsoons in the SCS. In this study, we present foraminifer SST esti-

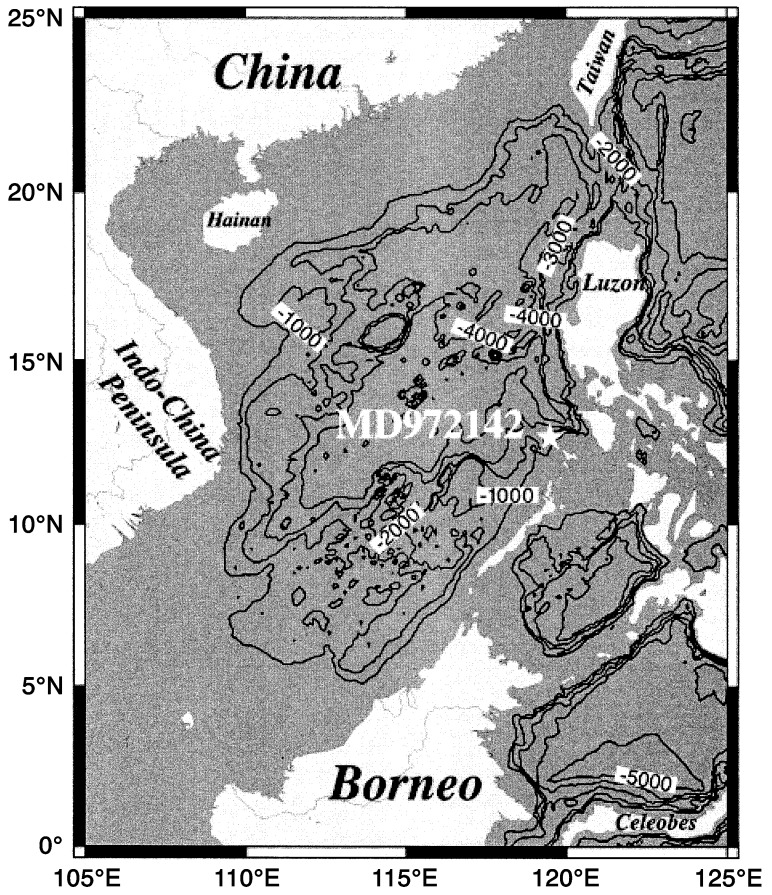

Fig. 1. Map showing the position of the IMAGES core MD972142.

mates and biogenic sediment productivity proxies from this record, spanning ~the past 500 000 years. The specific objectives of this study were to: (1) document variations in planktic foraminifer faunal SSTs and productivity-related biogenic sediment component concentrations and MARs in the SCS over the past 500 000 years; (2) determine the timing and magnitude of variations in the fauna SST and biogenic sediment productivity estimates associated with glacial–interglacial changes; (3) identify possible regional climatic processes (for example, East Asian monsoons) which may have affected both the SST and productivity changes in the SCS; and (4) compare paleomonsoon records of the SCS and the Arabian Sea, Indian Ocean.

2. Data and methods

For the purposes of this study, an IMAGES core (MD972142 (12°41.133′N, 119°27.90′E; water depth 1557 m)) was obtained from the western continental slope of Palawan Island, in the southwestern SCS (Fig. 1) by the French research vessel *Marion Dufresne* on its 1997 IMAGES III cruise (Chen et al., 1998). The sediments in this core are composed of light olive gray muds to foraminifer nannofossil oozes, interrupted by 18 visually distinguishable thin tephra layers. The thickness of these tephra layers ranges from 0.5 to 10 cm, with most >1 cm. The water depth for taking this core was well above the regional lysocline (~3500 m, Thunell et al., 1992), which en-

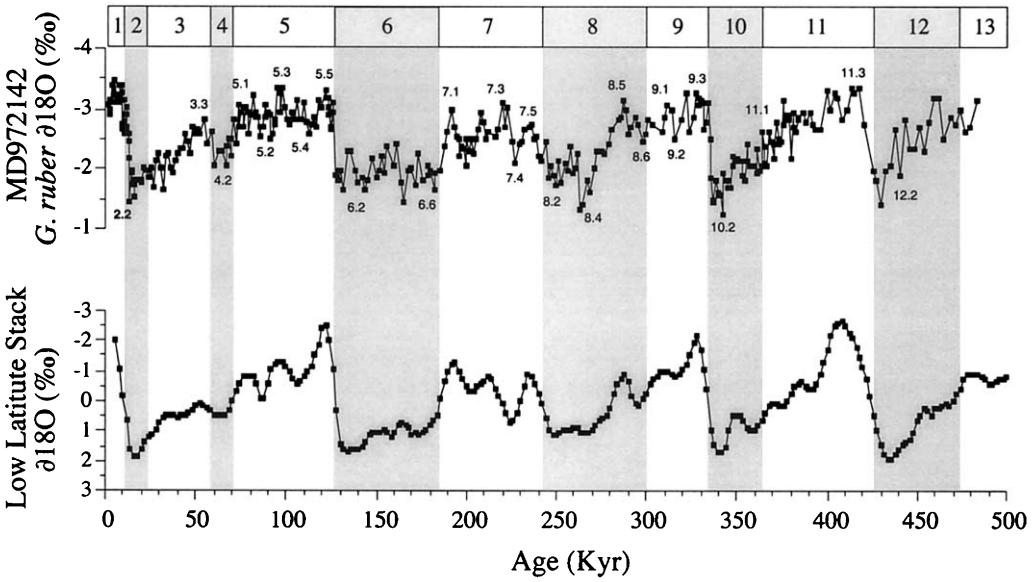

Fig. 2. The oxygen isotope (*Globigerinoides ruber*) stratigraphies of the IMAGES core MD972142 which is estimated to represent early stage 13 through the Holocene. The age control points are determined by comparing the curve of MD972142 $\delta^{18}O$ and a low-latitude stack (Bassinot et al., 1994).

sures good carbonate preservation at this site. The core was sampled every 4–12 cm and a total of 300 samples were analyzed for planktic foraminifer faunal assemblages, 353 samples for planktic foraminifer oxygen and stable carbon isotopes (*Globigerinoides ruber*), and 560 samples for biogenic carbonate and organic carbon concentration analysis. The intervals containing tephra layers were not used.

The 353 stable isotope measurements of the planktic foraminifer *Globigerinoides ruber* (white morphotype with size range 250–300 μm) were made at National Taiwan University using a Finnigan Delta Plus mass spectrometer with a Kiel automated carbonate device. Analyses were duplicated for every sample with a precision of 0.08‰ PDB. Average values from the screened duplicated results were then calculated (Fig. 2). Construction of the stratigraphy of core MD972142 was mainly based on a comparison of the planktic foraminifer $\delta^{18}O$ data from this core with a low-latitude $\delta^{18}O$ stack (Bassinot et al., 1994) (Fig. 2) and on the last appearance datum of *G. ruber* (pink morphotype) of ~120 000 years ago (Thompson et al., 1979) based on biostratigraphic examination on this core. The planktic foraminifer faunal census data were processed using standard techniques that have been applied in many previous SCS sediment studies (Chen et al., 1998, 1999; Chen and Huang, 1998) conducted at the Laboratory of Paleoceanography, National Taiwan Ocean University. The planktic foraminifera were picked from splits of the >150-μm size fraction containing approximate 300 specimens. A total of 27 faunal species were identified and the relative abundance of each species is expressed as a percentage of the total faunal assemblage (Fig. 3). The dominant species identified in this core were: *G. ruber*, *Neogloboquadrina dutertrei* (+*Neogloboquadrina pachyderma* (right coiling)), *Globigerinoides sacculifer*, *Globigerina calida*, *Pulleniatina obliquiloculata* and *Globigerinita glutinata*.

We estimated the SST by using a planktic foraminifer transfer function method. This statistical approach utilizes regression equations that relate modern coretop faunal distributions to overlying surface water temperatures (Imbrie and Kipp, 1971). In the western Pacific, SST estimates have historically been based on an old-version linear

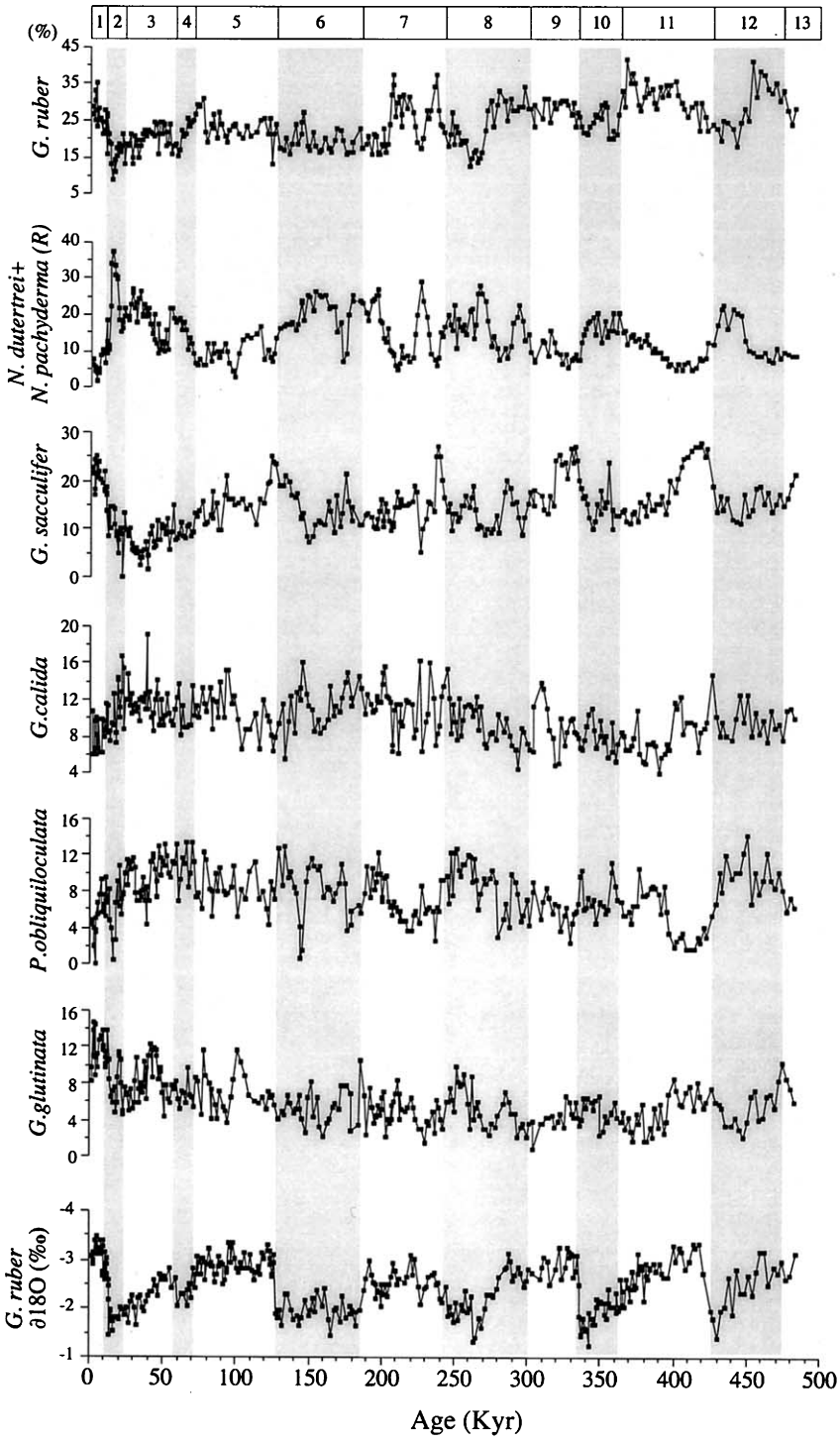

Fig. 3. Relative abundances of six dominant species of planktic foraminifera for core MD972142, plotted against age and compared to downcore $\delta^{18}O$ stratigraphy. Shaded intervals indicate glacial periods.

transfer function FP-12E (Thompson, 1981). This set of transfer functions has previously been applied in a project that estimated the LGM SST patterns of the western Pacific (CLIMAP, 1981). A methodologically different technique, SIMMAX-28 (Pflaumann et al., 1996), has been tested recently for estimating SCS SST records (Pflaumann and Jian, 1999; Jian et al., 2001). Since such paleo-SST estimates in the western Pacific may yield erroneous results due to no-analog problems, we attempted to use a revised method (Mix et al., 1999) to generate a transfer function for extracting paleo-SST signals from planktic foraminifer abundance data. The revised method consists of two steps. First, the procedure involves defining foraminifer Q-mode factor assemblages in MD972142 300 downcore samples, which resulted in two factors that represented 95% of the variance of the downcore faunal data. These two factors were: factor 1 (*Globigerinoides ruber*, *Globigerinoides sacculifer*; 51% of the variance) and factor 2 (*Neogloboquadrina dutertrei*+*Neogloboquadrina pachyderma* (right coiling); 44% of the variance). Next, the loadings of these two factors were mapped onto published western Pacific and SCS coretop data (Prell, 1985; Chen and Prell, 1998; Ho et al., 1998; Pflaumann and Jian, 1999) and the coretop samples with factor communalities <0.6 were excluded. The remaining 459 coretop samples (communalities >0.6) were then used as a calibration data set to generate transfer functions for estimating SSTs (Yu, 2000). The root mean square (RMS) errors of estimated cold (January)- and warm (July)-season SSTs in the equations are 2.3°C and 1.4°C respectively, somewhat larger than those in previous estimation methods. The larger RMS errors shown in the revised transfer function method result from the fact that factor assemblages were defined based on downcore samples and not specifically tuned to fit the coretop samples (Mix et al., 1999). We felt that this revised method might improve the accuracy of our SST estimates for the SCS records, as in Mix et al.'s (1999) experiments with equatorial Atlantic and eastern Pacific data sets, in which the discrepancy in estimating LGM tropical cooling between data and model appears to have been solved.

The 560 analyses for biogenic carbonate and organic carbon concentrations were conducted at National Taiwan Ocean University (Fig. 4). The samples were crushed to a fine powder after drying at 50°C and split into several sub-samples for analysis. We measured the total carbon content (TC) of the samples with a HORIBA EMIA-8210 carbon analyzer. The procedure involves heating the samples to $\sim$1300°C and measuring the combustion product CO_2 gases by gas chromatography. The resulting precision was $\pm 0.8\%$ of the values being measured. The carbonate content of the samples was determined by a fuming method. HCl was used to remove the carbonate content (TIC (total inorganic carbon)) of separate sub-samples. After the acid reaction, the sub-samples were repeatedly analyzed for remaining carbon content by the combustion method using the carbon analyzer. The carbonate content (TIC) could thus be calculated by subtracting total organic carbon (TOC) from the TC values. In order to avoid forcing apparent anti-correlation in percentage data, we calculated carbonate and TOC MARs (mg/cm^2/kyr) (Fig. 4) based on the following equation: $\mathrm{MAR} = \mathrm{SR} \times [\mathrm{BD} - (P \times \mathrm{WD})] \times \mathrm{wt}\%$ (Sykes and Ramsay, 1995). In this equation, SR is the linear sedimentation rate, BD is the wet bulk density (g/cm^3) measured from ship-board MST (multi-sensor track) equipment, and WD is the seawater density ($=1.025$ g/cm^3). P (%) is the estimated porosity of carbonate or TOC sediments. For calculating carbonate and TOC MARs, P was estimated with the following equation: $P = 0.72–0.045 \times Z$ (Simmons, 1990). Z (km) represents the depth of the core. When calculating sedimentation rate, and carbonate and TOC MARs, we found anomalously high values present in the upper part of the core down to a possibly maximum depth of about oxygen isotope stage 3 (Fig. 4). These anomalous MAR values may have resulted from a stretching of the upper part of the sediments collected with the giant piston core CALYPSO on board the RV *Marion Dufresne* (Szeremeta et al., 2000), and were not interpreted to reflect surface ocean variability in this study.

For spectral and cross-spectral analyses, the Mac user program ARAND (distributed by

Brown University) was used. The spectra were calculated by the Blackman–Tukey method (Jenkins and Watts, 1968) as used in SPECMAP studies (Imbrie et al., 1992, 1993).

3. Results

The $\delta^{18}O$ record of the surface water dwelling species *Globigerinoides ruber* follows closely the variations of the low-latitude $\delta^{18}O$ stack (Bassinot et al., 1994) (Fig. 2). The planktic foraminifer record documents six glacial–interglacial cycles, with large amplitudes varying from ~2.0‰ (stage 1/2, 9/10, and 11/12 transitions) to 1.4‰ (stage 7/8 transition). The oldest part of the record included in this study is at the uppermost end of stage 13; it is estimated to date to ~500 000 years ago. Sedimentation rates of this core are estimated to be ~5 cm/kyr (Fig. 4), with no significant variation between glacial and interglacial periods. These sedimentation rates are estimated here consistently with those reported from an eastern SCS core study (Thunell et al., 1992). The anomalous high values of sedimentation rates in the uppermost part of the core again could have been caused by stretching during the operation of the CALYPSO piston coring system.

The relative abundances of six dominant planktic foraminifer species are presented here in order to examine changes in sea-surface conditions, and climate changes in the southeastern SCS (Fig. 3). We observed large downcore variations in the relative abundances of these dominant species, indicating that considerable change in the surface water has occurred in this region over the past 500 000 years. The species abundance patterns contain major low-frequency glacial–interglacial and also high-frequency variations. For example, the abundances of a warm-water, deep mixed-layer species *Globigerinoides ruber* increased noticeably during glacial (stage 4, 8, 12) and interglacial periods (stage 1, 7, 9, 11) and reached a maximum in late stage 11 and early stage 12. Although the abundances of a cold-water, high productivity/upwelling indicator species *Neogloboquadrina dutertrei* showed high values during most glacial periods (stages 2, 4, 6, 8, 10, 12), there were also some peak values during interglacial periods (stages 3 and 7). The abundances of the other species also showed abundance maxima in both glacial and interglacial stages, and fluctuated in a high-frequency mode. The faunal abundance patterns suggest an instability in the surface ocean system of the SCS during the late Quaternary.

The planktic foraminifer SST estimates vary between 23.0°C and 26.5°C for the cold season (January) and between 27.4°C and 29.2°C for the warm season (July) over the past 500 000 years. The amplitudes of the SST changes (3.5°C and 1.8°C) observed in this record easily exceed the estimation errors (2.3°C and 1.4°C) in cold- and warm-season equations. The coretop values of the seasonal SSTs were ~26.5–29°C, in agreement with the approximate range ~27–29°C of modern SST observations at this site (NOAA, 1994). The estimates for LGM cooling at this site based on this record are ~3°C (January), which appears to be of the same magnitude as the cooling reported previously based on U^{k}_{37} records (Huang et al., 1997a,b; Pelejero et al., 1999a,b). However, they are smaller than those based on planktic foraminifer faunal estimates (~6°C) (Chen and Huang, 1998; Chen et al., 1999) obtained by using a global transfer function (Ortiz and Mix, 1997). This suggests that the revised transfer function method (Mix et al., 1999) adopted in this study produces more consistent estimates with those reported from previous studies, as the revised procedure better describes the total downcore faunal variation and more properly relates the faunal variation to local oceanographic processes. The 3°C magnitude of tropical LGM cooling that we estimated here also seems to be consistent with that reported in a recent re-evaluation (Schneider et al., 2000) and with that obtained through modeling (Hostetler and Clark, 2000).

The 500 000-year record generally exhibits a pattern of glacial decreases and interglacial increases in the faunal transfer function SST estimates, but with several exceptions of large-amplitude cooling during interglacial periods and warming events within glacial periods. For example, several cooling events were observed in inter-

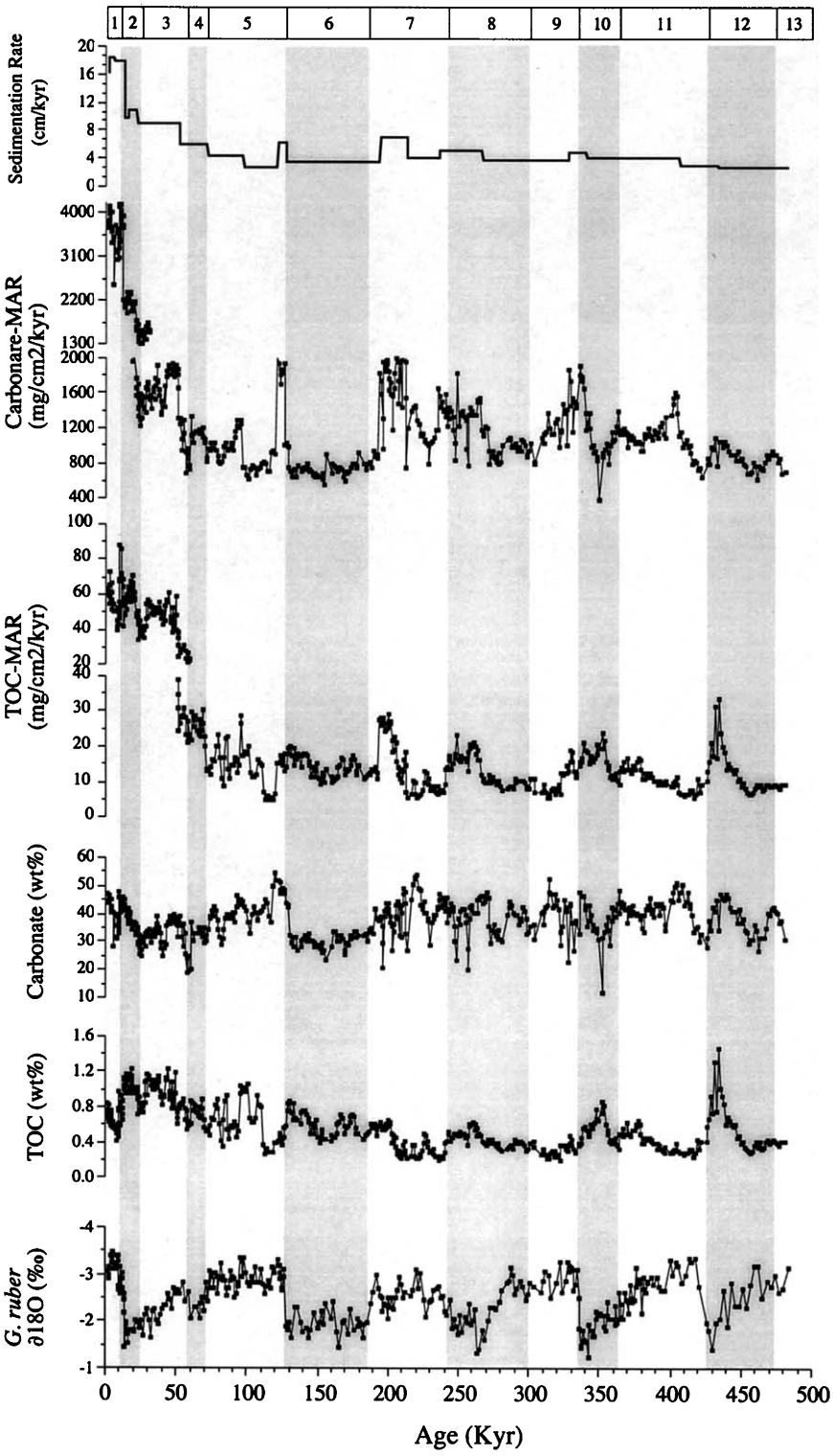
1
2
3
4
5
6
7
8
9
10
11
12
13
Sedimentation Rate (cm/kyr)
Carbonare-MAR (mg/cm2/kyr)
TOC-MAR (mg/cm2/kyr)
Carbonate (wt%)
TOC (wt%)
G. ruber ∂18O (‰)
0
50
100
150
200
250
300
350
400
450
500
Age (Kyr)

glacial stages 5 and 7; and some warming episodes occurred in glacial stages 6, 8, and 12 (Fig. 5). All of these episodes indicate that the surface ocean temperature variability in the SCS during the past 500 000 years was driven by more complicated factors than simply ice-volume forcing. Based on this record, we observed that large cooling spikes in this time series are near or close to the time intervals 10–60 ka, 140–150 ka, 250–260 ka, 340–360 ka, and 430 ka; some extreme warming events lie close to the intervals 50 ka, 70–95 ka, 120 ka, 170 ka, 210 ka, 235 ka, 280 ka, 320 ka, and 370–420 ka. Superimposed on the high-frequency variations, the SST records are characterized by more frequent and abrupt cooling events beginning ~250 000 years ago. Large cooling events appear to be more evident after glacial stage 8 and become much more intensified in stage 2–4. Overall, the SST records are not well-correlated with glacial and interglacial cycles.

Unlike SST variations, the carbonate concentration record of MD972142 exhibits significant variation at the broad glacial–interglacial cycles characteristic of the *Globigerinoides ruber* $\delta^{18}O$ time series (Fig. 4). The carbonate content makes up ~15–55 wt% of the MD972142 sediments, usually with maxima in interglacial and minima in glacial periods. The MD972142 carbonate record is consistent with that of a nearby core (GGC-9 (1465 m)) from the Palawan slope (Thunell et al., 1992). Several spikes of low carbonate content are located near the intervals of tephra layers that are not sampled for the carbonate analyses. The downcore pattern of carbonate content corresponds to previously reported SCS carbonate sedimentation patterns from depths above the regional lysocline where terrigenous inputs are thought to be dominant (Thunell et al., 1992; Wang et al., 1995; Chen et al., 1997). In attempting to minimize the problems of terrigenous dilution and other biogenic components, we have quantified the variability of carbonate flux into the sediment by calculating carbonate MARs (Fig. 4). In the uppermost part of the record, the carbonate MARs show anomalously high values which are presumably associated with the stretching of the core. From the depth at stage 3 to the bottom of the record, the carbonate MARs vary between ~500 and 2000 mg/cm^2/kyr, with high values centered primarily in interglacial periods (with an exception in stage 5) or in glacial–interglacial transitions. The peaks in carbonate MARs during glacial–interglacial transitions are evident during stage 5–6, 7–8, and 9–10 transitions, and are most likely due to changing preservation. Many earlier observations (Peterson and Prell, 1985; Thunell et al., 1992; Chen et al., 1997) on Indian Ocean or SCS cores indicated a presence of carbonate preservation spikes during deglaciation stages. Given the close correspondence between our calculated carbonate MAR and content, the first-order variations of the carbonate MARs are probably driven by glacial–interglacial productivity and/or carbonate preservation changes in the SCS. As productivity in the SCS during interglacial stages is not likely high (Thunell et al., 1992) and the preservation level in the Indo-Pacific Ocean during interglacial stages is generally lower than that in glacial, the carbonate MAR and content variation patterns seem likely to indicate the changing terrigenous sediment supplies which are associated with glacial–interglacial sea-level fluctuations in the SCS.

TOC concentrations constitute ~0.2–1.4 wt% of the sediments, with maxima usually in glacial periods and minima typically in interglacial periods (Fig. 4). The glacial–interglacial variations in TOC content have also been reported from nearby short gravity cores and have been used to demonstrate high glacial productivity in low-latitude surface oceans (Thunell et al., 1992). The general downcore pattern of the TOC maxima and minima exhibits more low-frequency variability than

Fig. 4. Sedimentation rate, carbonate MAR, TOC MAR, and carbonate and TOC concentrations measured in sediment samples from core MD972142, plotted against age and compared to downcore $\delta^{18}O$ stratigraphy. Shaded intervals indicate glacial stages. Anomalously high values shown in the sedimentation rate and MAR are caused by the stretching of the uppermost part of the core.

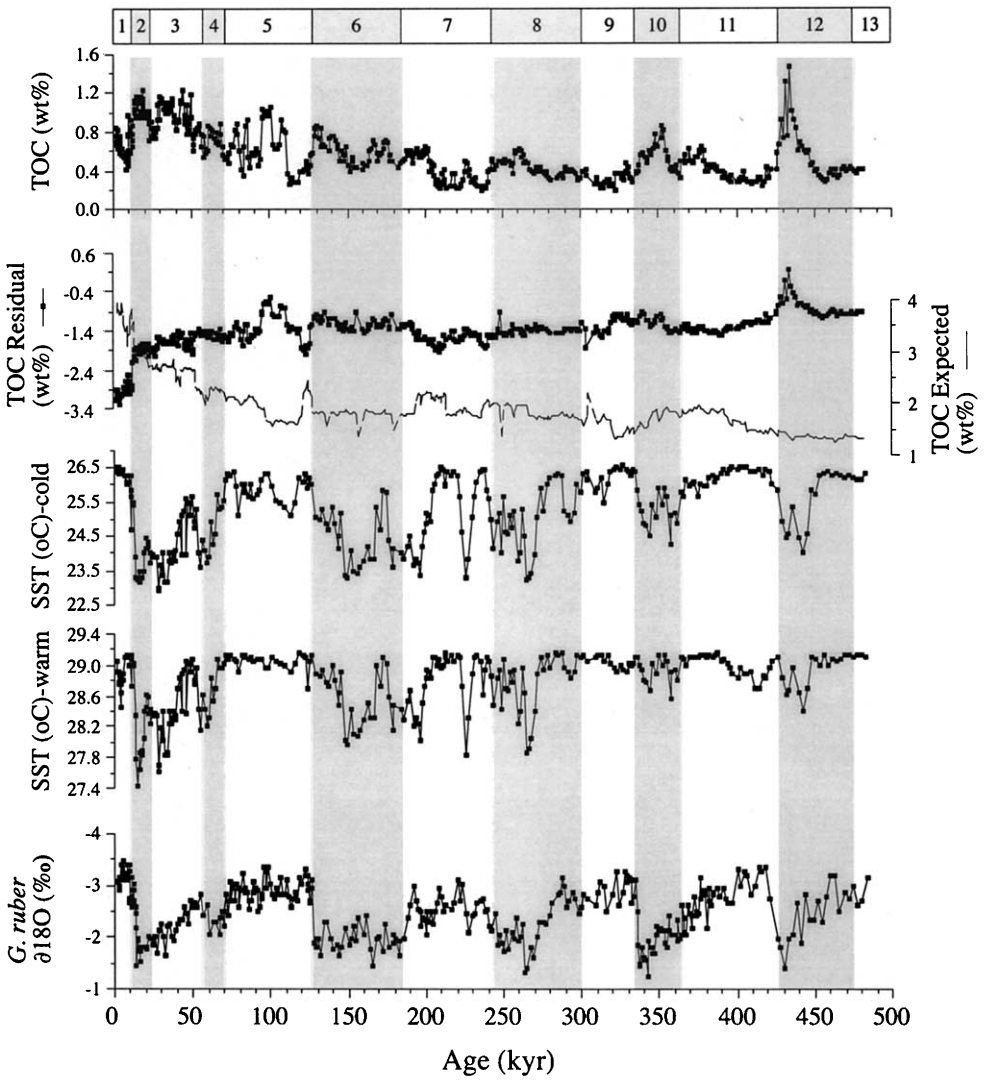

Fig. 5. Measured TOC concentrations, calculated TOC concentrations at constant productivity (147 g C/m^2/yr; San Diego-McGlone et al., 1999) and variable sedimentation rates (TOC expected, thin line), difference between measured and calculated TOC concentrations (TOC residual = measured minus calculated TOC, dotted line), and SSTs for cold- and warm-season estimates by planktic foraminifer transfer functions from core MD972142, plotted against age and compared to downcore δ^{18}O stratigraphy. Shaded intervals indicate glacial stages.

that shown in the carbonate records. In addition to a maximum event centered on ~430 ka, the record also shows a long-term trend with increased TOC content since 400 000 years ago. Over the broad, low-frequency curve of the TOC content variations, intervals with high values are observed from ~10–60 ka, 95–110 ka, 140–150 ka, 250–260 ka, 340–360 ka, and at 430 ka. These high TOC events seem to occur during the later stages of glacial periods. When converting the TOC content into TOC flux (a proxy indicator for surface productivity), our calculations show that, in spite of the fact that the uppermost part of the record is affected by stretching of the core, the TOC MARs (Fig. 4) vary between ~5 and 30 mg/cm^2/kyr and match

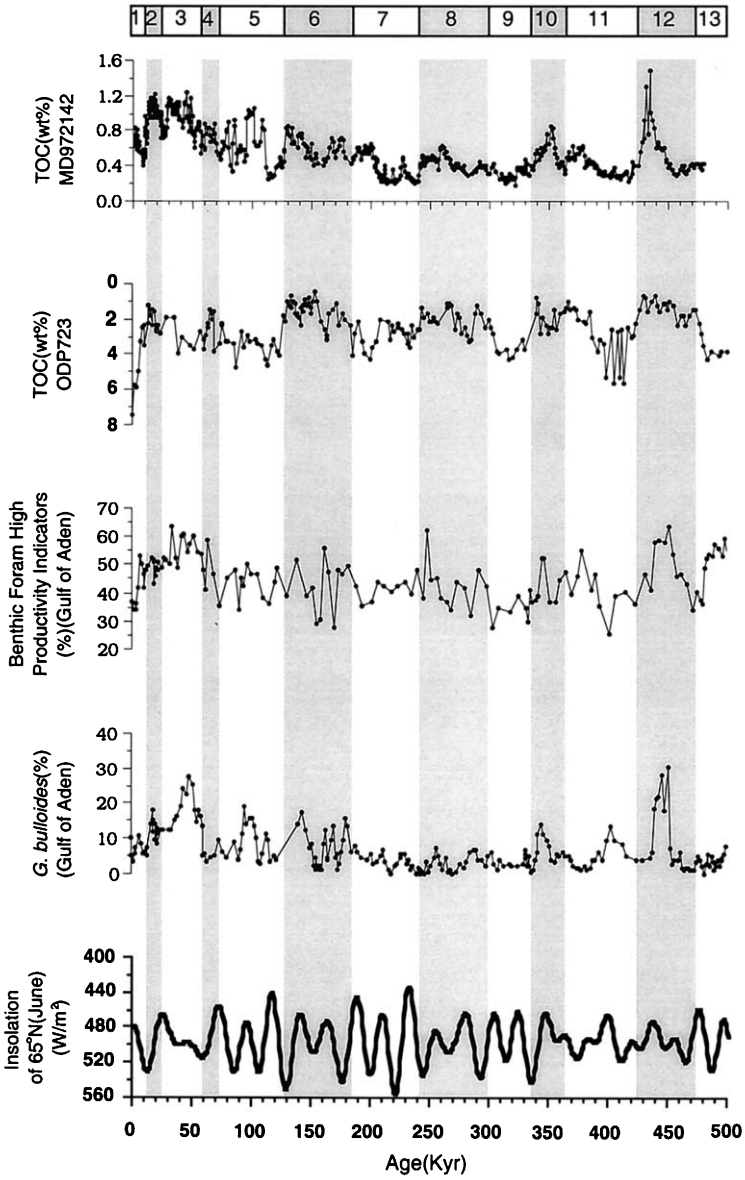

Fig. 6. Comparisons of MD972142 TOC, ODP 723 TOC (summer monsoon proxy) (Emeis et al., 1995) from the Arabian Sea, and Gulf of Aden benthic productivity and *G. bulloides*% (winter monsoon indicators) (Almogi-Labin et al., 2000) records.

well the variations of TOC content. Several high TOC intervals, for example, from ~200 ka, 250–260 ka and 340–360 ka, become more pronounced in the MAR curve. Increasing sedimentation rates have also been thought to enhance TOC preservation (Müller and Suess, 1979; Sarnthein et al., 1988). When assessing past surface ocean productivity changes, the pattern of TOC content seems to provide more reliable results than do TOC MARs. In subsequent analyses, our interpretation of the biogenic components of MD972142 will be primarily based on concentration records.

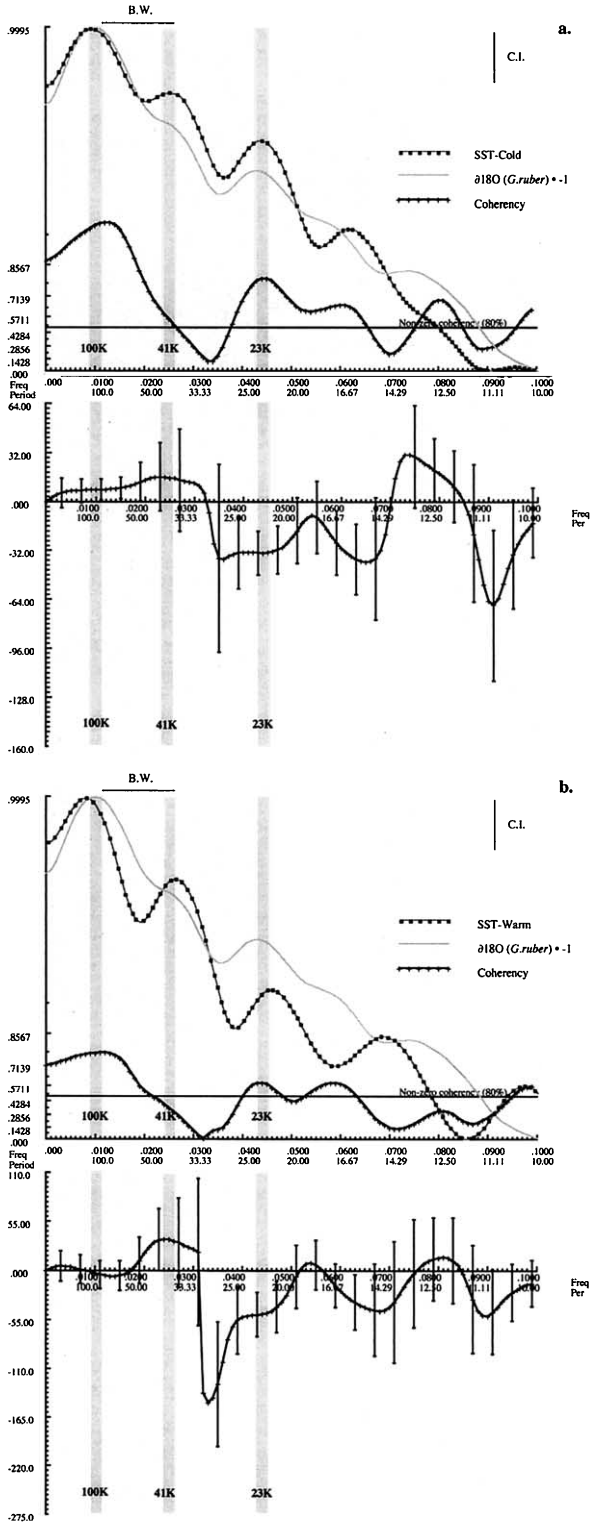
B.W.
a.
C.I.
SST-Cold
∂18O (G.ruber) • -1
Coherency
Non-zero coherency (80%)
100K
41K
23K
Freq
Period
Freq
Per
b.
SST-Warm
∂18O (G.ruber) • -1
Coherency
Non-zero coherency (80%)
100K
41K
23K

4. Discussion

The records of planktic foraminifer SSTs and TOC-based productivity indicators from core MD972142 indicate significant fluctuation during the past 500 000 years. Since the SCS is a marginal sea of the western Pacific, the SST, surface circulation, and biogenic sedimentation in the SCS must be affected by sea-level changes (Wang et al., 1999a,b). During times of lowered sea-level (glacials), the SCS SST may have decreased because the surrounding continental shelves of the SCS emerged and restricted the inflow of warm surface waters from low-latitude oceans. Moreover, more down-slope or laterally advected sediment transports may occur during glacial periods due to the redistribution of sediments in response to sea-level changes. When interpreting the MD972142 records in terms of past monsoon variability, it is necessary to understand how much of the variation exhibited in the records is due to changes in sea-levels. As shown in the carbonate record (Fig. 4), glacial parts of the sediment core are characterized by relatively low carbonate content. The core site is presently located at a water depth of 1557 m, which is well above the regional lysocline (~3500 m) and also above an estimated glacial lysocline depth (~2500 m), based on abundance data of pteropods in gravity cores collected from a bathymetric transect along the Palawan slope (Thunell et al., 1992). Glacial–interglacial changes in carbonate preservation do not seem to be effective in modifying the carbonate content of the core. Moreover, as carbonate preservation and productivity levels are both enhanced during glacial periods in the Pacific (Farrell and Prell, 1989; Sarnthein et al., 1988), all instances indicate that the glacial low carbonate content shown in core MD972142 was most likely driven by increased terrigenous sediment dilution effects. Increased siliceous component concentrations are also not possibly responsible for the dilution effects, since siliceous fossils (diatoms and radiolarians) are rare in these sediment samples. Since this site is located far away from the large rivers that drain into the SCS, transport of riverine sediments to this site by lateral advection may not be significant. We inferred that the increased terrigenous inputs are primarily caused by local redistribution of sediments along the shelf-slope profile of the Palawan. More terrigenous material may have been brought by various down-slope transfer processes, when sea-level fell during glacial periods. A sea-level reconstruction in the SCS based on changes in shoreline sedimentary facies appears to be parallel to global records (Hanebuth et al., 2000). Recent U_k^{37} studies (Pelejero et al., 1999a,b; Kienast et al., 2001) using SCS cores also suggest a synchronized relationship between SCS SST and high-latitude climate change. By accepting the premise that sea-level effects left their imprint on the MD972142 records, the first-order variations exhibited in the SST and TOC and characterized in terms of glacial and interglacial cycles may be partially attributable to sea-level fluctuations in the SCS.

Atmospheric circulation changes may also play a role in controlling glacial SCS SST and TOC. When we examined the SST and TOC records together (Fig. 5), we found that the glacial periods were characterized by relatively low SSTs and high TOC content, indicating cooling and high productivity conditions in surface oceans. Previous studies on SCS marine records (Chen and Huang, 1998) and Chinese loess (Ding et al., 1994, 1995) have already pointed out the importance of ice-volume forcing in determining the intensity of East Asian winter monsoon winds, via a mechanism of latitudinal shifting position and/or strength of Siberian high-pressure systems. Large-scale glaciation in the continents of the

Fig. 7. Cross-spectral analysis between MD972142 estimated SST for cold- and warm-seasons, and the planktic foraminifer *Globigerinoides ruber* $\delta^{18}O$ for global ice-volume estimates. Notice that the $\delta^{18}O$ was multiplied by -1 to transform the interglacial values into positive and glacial values into negative. Three major orbital frequency bands are shaded (100 kyr^{-1}, 41 kyr^{-1}, and 23 kyr^{-1}), in which statistically significant coherencies between these two time series and the phase relationships of SST relative to changes in the global ice volume are shown.

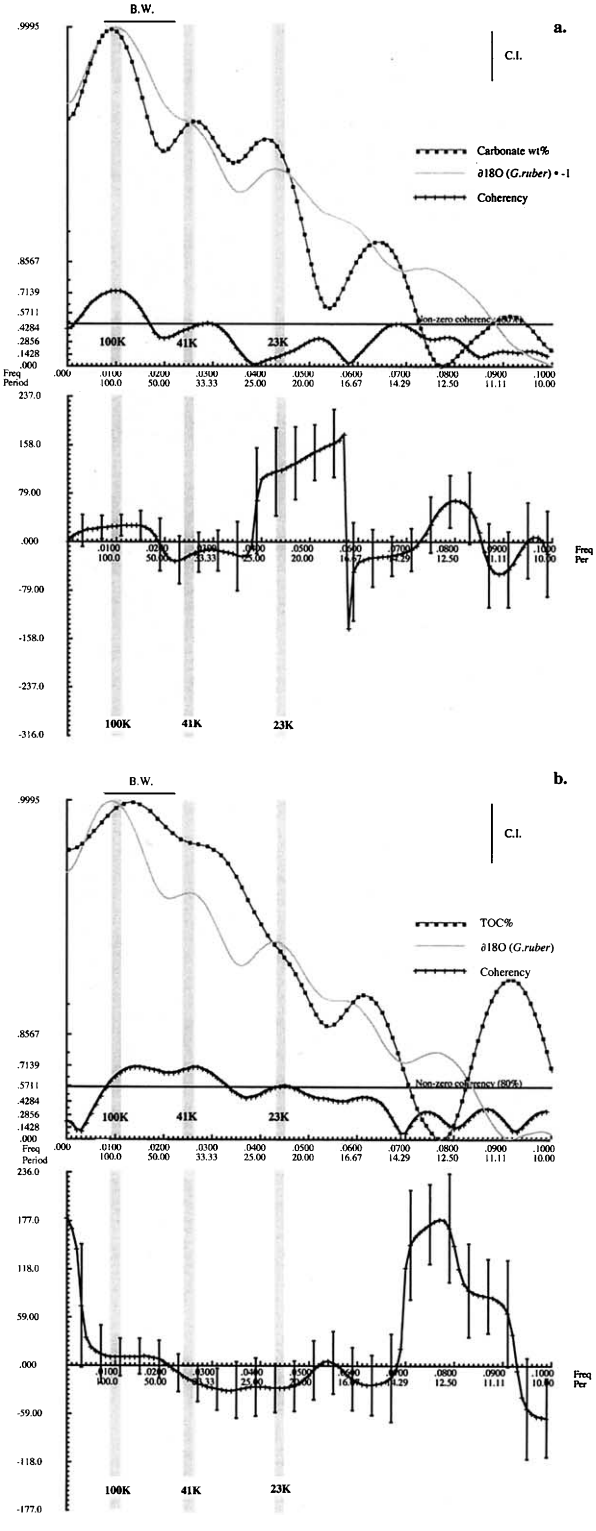
a.
B.W.
C.I.
Carbonate wt%
∂18O (G.ruber) • -1
Coherency
Non-zero coherency (95%)
100K
41K
23K
Freq
Period
b.
B.W.
C.I.
TOC%
∂18O (G.ruber)
Coherency
Non-zero coherency (80%)
100K
41K
23K
Freq
Period

Northern Hemisphere may intensify the high-pressure systems, which in turn bring more cold northeasterly winds to the SCS. The low SSTs and high productivity observed during the glacial periods of the MD972142 record may also reflect strong wind-induced mixing, and nutrient enrichment with high productivity (Ittekkot et al., 1992).

Some rapid, high-frequency oscillations shown in the SST and TOC records which do not closely parallel the $\delta^{18}O$ curve could be due to other forcing mechanisms. Because high TOC content may result from increased sedimentation rates that enhance TOC preservation, the influences of sedimentation rate changes on TOC content must be estimated. To this end, we calculated expected TOC content resulting under conditions of constant productivity and varied sedimentation rates by an equation: TOC expected $(\%) = (0.0030 \times R \times S^{0.30})/p_s$ (Müller and Suess, 1979) (Fig. 5). R represents the observed regional productivity in the SCS (147 g C/m^2/yr; San Diego-McGlone et al., 1999). S is the estimated sedimentation rate (cm/kyr) for the core, and p_s is the estimated dry bulk density for the core. This calculation yields changes in TOC content of less than $\sim$1%, estimated from varied sedimentation rate and constant productivity at the site of core MD972142. The large increases in expected TOC content in the uppermost part of the core are due to core stretching. Subtracting the expected TOC content of constant productivity from the measured TOC content yields a record of residual TOC content, which is attributable to changing productivity. The residual record preserves TOC content variation of similar timing but rather damped amplitude. Examining the SST and TOC together, we found several periods of relatively low SST and high productivity at 10–60 ka, 95–110 ka, 140–150 ka, 250–260 ka, 340–360 ka, and at 430 ka. These intervals seem to reflect more intensified winter monsoon winds in the SCS. Even more interesting, these intervals correspond to events of stronger winter monsoons over the Arabian Sea, based on a record of the planktic foraminifer *G. bulloides* abundances and benthic foraminifer productivity indices in a core from the Gulf of Aden (Almogi-Labin et al., 2000) (Fig. 6). The Gulf of Aden is a semi-enclosed gulf, which receives little influence from the summer monsoon upwelling prevailing in the Arabian Sea. During winter monsoon seasons, the surface waters in the Gulf of Aden experience cooling and mixing, with nutrient-rich subsurface waters injected into the photic zones. Therefore, the Gulf of Aden core records Indian Ocean winter monsoon variability (Almogi-Labin et al., 2000). Because the age model of this core was constructed based on the SPECMAP time scale, correlation between events registered in both records is considered to be accurate. In addition, several intervals are characterized by relatively high SST and low productivity at 50 ka, 70–95 ka, 120 ka, 170 ka, 210 ka, 235 ka, 280 ka, 320 ka, and 370–420 ka. Calculations of monthly averaged wind-stress field and divergence of Ekman transport (Hellerman and Rosenstein, 1983) show downwelling and deepened mixed-layer conditions present off the coast of the northwestern Palawan during July, the summer monsoon season in the SCS. These intervals appear to indicate short episodes of intensified summer monsoon winds in the SCS. Comparing our records to many previously published Indian Ocean summer monsoon reconstructions, we found that the variation patterns shown in these records have a similar structure in terms of timing of intensified summer monsoons. (Some are of relatively low resolution; see: Clemens et al., 1991; Murray and Prell, 1992; Anderson and Prell, 1993.) The correspondences be-

Fig. 8. Cross-spectral analysis between MD972142 carbonate and TOC concentrations, and the planktic foraminifer *Globigerinoides ruber* $\delta^{18}O$ for global ice-volume estimates. Notice that for carbonate spectra, the $\delta^{18}O$ was multiplied by -1 to transform the interglacial values into positive and glacial values into negative. Three major orbital frequency bands are shaded (100 kyr^{-1}, 41 kyr^{-1}, and 23 kyr^{-1}), in which statistically significant coherencies between these two time series and the phase relationships of the carbonate and TOC concentrations relative to changes in the global ice volume are shown.

tween these two records are especially evident over the intervals 50 ka, 70–95 ka, 120 ka, and 210 ka. The strong summer monsoon intervals identified from the MD972142 record match very well, with a more high-resolution summer monsoon indicated by the U_k^{37} and TOC record from Arabian Sea ODP Site 723 (Emeis et al., 1995) (Fig. 6). By combining all the correlations found in the records from the SCS and the Arabian Sea, it is possible to infer that the MD972142 records contain a mix of influences from both winter and summer monsoons. The coincidence of intensified winter and summer monsoon events expressed in both the SCS and Arabian Sea data indicates more regionally effective patterns of the Asian monsoon system. This comparison also suggests that there are coherent patterns of temporal changes in different parts of tropical monsoon-affected areas over glacial–interglacial time scales.

We performed spectral and cross-spectral analyses to evaluate the dominant periodicities apparent in the MD972142 records. We also looked at the coherent and phase relationships between the records and global climate change over orbital time scales (10^4–10^5 years). In the variance density spectra of the SSTs (Fig. 7), statistically significant variance peaks occur at all orbital frequency bands (100 kyr^{-1}, 41 kyr^{-1}, and 23 kyr^{-1}). The presence of a 100-kyr periodicity in the MD972142 SST records suggests an ice-volume- and/or sea-level-related forcing on SCS monsoon changes. The dominances of 41 kyr and 23 kyr in the SST records imply an orbitally driven solar insolation influence on the SCS monsoon systems, as previously proposed in Indian Ocean monsoon studies (Clemens et al., 1991). The phase relationships between the SST and *Globigerinoides ruber* $\delta^{18}O$ (ice-volume indicator) records from the same core analyzed by cross-spectral analyses (Fig. 7) reveal consistent scenarios. Significant coherencies are observed at 100-kyr^{-1} and 23-kyr^{-1} frequency bands. Maximum MD972142 SSTs are nearly in-phase with minimum ice volumes over 100-kyr cycles, indicating a response to glacial boundary conditions (Anderson and Prell, 1993; Ding et al., 1995; Chen and Huang, 1998). The maximum SSTs lag minimum ice volume by ~3000–4000 years at 23-kyr cycles. Others have reported the same phase lagging of Indian Ocean summer monsoon intensities in this cycle, although at different magnitudes of phase lags (Clemens et al., 1991).

For carbonate content records, spectral analyses (Fig. 8a) indicated statistically significant variance peaks in all three orbital frequency bands. Using cross-spectral analysis, we found that the carbonate record is strikingly coherent and in-phase with ice-volume changes at 100-kyr cycles. Maximum carbonate contents are associated with minimum ice volume and/or high sea-level conditions. The peaks at 41-kyr^{-1} and 23-kyr^{-1} frequency bands shown in the carbonate record are indications of a combination of influences from sea-level, carbonate productivity and dissolution, or even more complicated factors, since no significant coherent and in-phase relationship is observed at these two frequency bands. The spectrum of the MD972142 TOC content (Fig. 8b) exhibits orbital and non-orbital peaks. At orbital frequency bands, the TOC variation shows a noticeable peak in the 100-kyr cycle. Maximum TOC contents are coherent and nearly in-phase with maximum ice volume at this frequency band. This suggests that the production and/or preservation of MD972142 TOC is primarily linked to sea-level or ice volume-induced winter monsoon wind effects. The non-orbital cyclicities (~70 kyr and 35 kyr) evident in the TOC record are also dominant in Indian Ocean summer monsoon records (Clemens and Prell, 1991) and equatorial Pacific eolian grain size and radiolarian divergence records (Pisias and Rea, 1988). The climatic linkages among the non-orbital cyclicities shown in these records, although requiring further investigation, suggest that more complex forcing mechanisms than previously thought may govern tropical climate variability over orbital time scales.

5. Conclusions

This study of planktic foraminifer faunal SST estimates and biogenic carbonate and TOC concentrations from an IMAGES core record from

the southeastern SCS near Palawan Island reveals that SSTs and TOC are good proxies for East Asian monsoon strength. The carbonate content record is dominated by terrigenous sediment inputs, indicating an environmental influence from sea-level fluctuations in this record. The record shows that glacial periods are usually characterized by relatively low SSTs and high TOC content, while interglacial periods are characterized by relatively high SSTs and low TOC content. This association provides an indication that the temperature and productivity levels in the surface ocean of the SCS are largely controlled by sea-level fluctuations and/or ice volume-induced atmospheric circulation changes in monsoon wind intensities in the SCS. Several short-lived, high-frequency oscillation intervals shown in SST and TOC records which are not parallel to the $\delta^{18}O$ curve are attributed to other forcing factors that control the monsoons. These intervals of intensified winter and summer monsoons can be traced beyond the SCS. When we compared the MD972142 record with Arabian Sea winter and summer monsoon variability reconstructions, we found a remarkably close correspondence. Moreover, the records from these two regions share a similar structure in terms of the timing of intensified monsoon winds. We infer that the MD972142 records contain combined influences from both winter and summer monsoons. The coincidence of intensified winter and summer monsoon events expressed in both the SCS and Arabian Sea indicates more regionally effective patterns of the Asian monsoon systems. The monsoon indices show strong peaks at three orbital frequency bands (100 kyr^{-1}, 41 kyr^{-1}, and 23 kyr^{-1}), suggesting that over orbital time scales, ice volume and orbital solar insolation changes are all possible mechanisms for controlling SCS monsoon variations. The SCS SST lags ice volume by $\sim$3000–4000 years at 23-kyr cycles, consistent with that reported from Arabian Sea summer monsoon records. Although this should also be tested by other proxies, our finding suggests a more regionally coherent temporal pattern of monsoon variations in the Indian Ocean and the SCS than previously assumed.

Acknowledgements

This research was supported by the National Science Council (NSC89-2611-M-019-032-IM), Academia Sinica (Asian Paleoenvironmental Changes (APEC) Projects), and National Taiwan Ocean University, Republic of China. We thank Hodaka Kawahata, Nick Pisias, and Franck Bassinot for their constructive reviews.

References

Almogi-Labin, A., Schmiedl, G., Hemleben, C., Siman-Tov, R., Segl, M., Meischner, D., 2000. The influence of the NE winter monsoon on productivity changes in the Gulf of Aden, NW Arabian Sea, during the last 530 ka as recorded by foraminifera. Mar. Micropaleontol. 40, 295–319.

Anderson, D.M., Prell, W.L., 1993. A 300 kyr record of upwelling off Oman during the late Quaternary: evidence of the Asian southwest monsoon. Paleoceanography 8, 193–208.

Bassinot, F., Labeyrie, L.D., Vincent, E., Quidelleur, X., Shackleton, N.J., Lancelot, Y., 1994. The astronomical theory of climate and the age of the Brunhes-Matuyama magnetic reversal. Earth Planet. Sci. Lett. 126, 91–108.

Chen, M.-T., Huang, C.-Y., Wei, K.-Y., 1997. 25,000-year late Quaternary records of carbonate preservation in the South China Sea. Palaeogeogr. Palaeoclimatol. Palaeoecol. 129, 155–169.

Chen, M.-T., Beaufort, L., the Shipboard Scientific Party of the IMAGES III/MD106-IPHIS Cruise (Leg II), 1998. Exploring Quaternary variability of the East Asian monsoon, Kuroshio Current, and the Western Pacific warm pool systems: high-resolution investigations of paleoceanography from the IMAGES III/MD106-IPHIS cruise. Terrestrial, Atmospheric and Oceanic Sciences 9, 129–142.

Chen, M.-T., Huang, C.-Y., 1998. Ice-volume forcing of winter monsoon climate in the South China Sea. Paleoceanography 13, 622–633.

Chen, M.-T., Prell, W.L., 1998. Faunal distribution patterns of planktonic foraminifers in surface sediments of the low latitude Pacific. Palaeogeogr. Palaeoclimatol. Palaeoecol. 137, 55–77.

Chen, M.-T., Wang, C.-H., Huang, C.-Y., Wang, P., Wang, L., Sarnthein, M., 1999. A late Quaternary planktonic foraminifer fauna record of rapid climatic changes from the South China Sea. Mar. Geol. 156, 85–108.

Clemens, S.C., Prell, W.L., Murray, D., Shimmield, G., Weedon, G., 1991. Forcing mechanisms of the Indian Ocean monsoon. Nature 353, 720–725.

Clemens, S.C., Prell, W.L., 1991. Late Quaternary forcing of Indian Ocean summer monsoon winds: a comparison of

Fourier model and general circulation model results. J. Geophys. Res. D 12, 22683–22700.

Climate: Long-Range Investigation, Mapping, and Prediction Member (CLIMAP), 1981. Seasonal reconstructions of the Earth's surface at the last glacial maximum. MAP and Chart Series MC-36. Geol. Soc. Am., Boulder, CO, pp. 1–18.

Ding, Z., Yu, Z., Rutter, N.W., Liu, T., 1994. Towards an orbital time scale for Chinese loess deposits. Quat. Sci. Rev. 13, 39–70.

Ding, Z., Liu, T., Rutter, N.W., Yu, Z., Guo, Z., Zhu, R., 1995. Ice-volume forcing of East Asian winter monsoon variations in the past 800,000 years. Quat. Res. 44, 149–159.

Emeis, K.-C., Anderson, D.M., Doose, H., Kroon, D., Schulz-Bull, D., 1995. Sea-surface temperatures and the history of monsoon upwelling in the Northwest Arabian Sea during the last 500,000 years. Quat. Res. 43, 355–361.

Farrell, J.W., Prell, W.L., 1989. Climatic change and $CaCO_3$ preservation: an 800,000 year bathymetric reconstruction from the central equatorial Pacific Ocean. Paleoceanography 4, 447–466.

Hanebuth, T., Stattegger, K., Grootes, P.M., 2000. Rapid flooding of the Sunda Shelf: A late-glacial sea-level record. Science 288, 1033–1035.

Hellerman, S., Rosenstein, M., 1983. Normal monthly wind stress over the world ocean with error estimates. J. Phys. Oceanogr. 13, 1093–1104.

Ho, C.-R., Zheng, Q., Soong, Y.-S., Kao, N.-J., Hu, J.-H., 2000. Seasonal variability of sea surface height in the South China Sea observed with TOPEX/Poseidon altimeter data. J. Geophys. Res. C 105, 13981–13990.

Ho, H.-W., Chen, M.-T., Zheng, L., Huang, C.-Y., 1998. A preliminary analysis on the distribution patterns of recent surface-sediment planktonic foraminifers and of upper-layer ocean environments in the South China Sea. J. Geol. Soc. China 40, 43–72.

Hostetler, S.W., Clark, P.U., 2000. Tropical climate at the last glacial maximum inferred from glacier Mass-Balance Modeling. Science 290, 1747–1750.

Huang, C.-Y., Liew, P.-M., Zhao, M., Chang, T.-C., Kuo, C.-M., Chen, M.-T., Wang, C.-H., Zheng, L., 1997a. Deep sea and lake records of the Southeast Asian paleomonsoons for the last 25 kyrs. Earth Planet. Sci. Lett. 146, 59–72.

Huang, C.-Y., Wu, S.-F., Zhao, M., Chen, M.-T., Wang, C.-H., Tu, X., Yuan, P.B., 1997b. Surface ocean and monsoon climate variability in the South China Sea since last glaciation. Mar. Micropaleontol. 32, 71–94.

Imbrie, J., Kipp, N.G., 1971. A new micropaleontological method for quantitative paleoclimatology: application to a late Pleistocene Caribbean core. In: Turekian, K.K. (Ed.), The Late Cenozoic Glacial Ages. Yale University Press, New Haven, CT, pp. 71–181.

Imbrie, J., Boyle, E.A., Clemens, S.C., Duffy, A., Howard, W.R., Kukla, G., Kutzbach, J., Martinson, D.G., McIntyre, A., Mix, A.C., Molfino, B., Morley, J.J., Peterson, L.C., Pisias, N.G., Prell, W.L., Raymo, M.E., Shackleton, N.J., Toggweiler, J.R., 1992. On the structure and origin of major glaciation cycles. 1. linear responses to Milankovitch forcing. Paleoceanography 7, 701–738.

Imbrie, J., Boyle, E.A., Clemens, S.C., Duffy, A., Howard, W.R., Kukla, G., Kutzbach, J., Martinson, D.G., McIntyre, A., Mix, A.C., Molfino, B., Morley, J.J., Peterson, L.C., Pisias, N.G., Prell, W.L., Raymo, M.E., Shackleton, N.J., Toggweiler, J.R., 1993. On the structure and origin of major glaciation cycles. 2. the 100,000-year cycle. Paleoceanography 8, 99–735.

Ittekkot, V., Nair, R.R., Honjo, S., Ramaswamy, V., Bartsch, M., Manganini, S., Desai, B.N., 1991. Enhanced particle fluxes in Bay of Bengal induced by injection of fresh water. Nature 351, 385–387.

Ittekkot, V., Haake, B., Bartsch, M., Nair, R.R., Ramaswamy, V., 1992. Organic carbon removal in the sea: the continental connection. In: Summerhayes et al. (Eds.), Upwelling Systems: Evolution Since the Early Miocene. Geological Society Special Publication No. 64, pp. 167–176.

Jian, Z., Huang, B., Kuhnt, W., Lin, H.-L., 2001. Late Quaternary upwelling intensity and East Asian Monsoon Forcing in the South China Sea. Quat. Res. 55, 363–370.

Jekins, G.M., Watts, D.G., 1968. Spectral Analysis and its Applications. Holden-Day, San Francisco, CA, 525 pp.

Kienast, M., Steinke, S., Stattegger, K., Calvert, S.E., 2001. Synchronous tropical South China Sea SST changes and Greenland warming during deglaciation. Science 291, 2132–2134.

Mix, A.C., Morey, A.E., Pisias, N.G., 1999. Foraminiferal fauna estimates of paleotemperature: circumventing the no-analog problem yields cool ice age tropics. Paleoceanography 14, 350–359.

Müller, P.J., Suess, E., 1979. Productivity, sedimentation rate, and sedimentary organic matter in the oceans I. Organic carbon preservation. Deep-Sea Res. 26A, 1347–1362.

Murray, D.W., Prell, W.L., 1992. Late Pliocene and Pleistocene climatic oscillations and monsoon upwelling recorded in sediments from the Owen Ridge, northwestern Arabian Sea. In: Summerhayes et al. (Eds.), Upwelling Systems: Evolution Since the Early Miocene. Geological Society Special Publication No. 64, pp. 301–321.

National Oceanic and Atmospheric Administration (NOAA), 1994. World Ocean Atlas 1994 CD-ROM data set documentation. U.S. Department of Commerce, 1–3, 1–35.

Ortiz, J.D., Mix, A.C., 1997. Comparison of Imbrie-Kipp transfer function and modern analogy temperature estimates using sediment trap and core top foraminiferal faunas. Paleoceanography 12, 175–190.

Pelejero, C., Grimalt, J.O., Sarnthein, M., Wang, L., Flores, J.-A., 1999a. Molecular biomarker record of sea surface temperature and climatic change in the South China Sea. Mar. Geol. 156, 109–121.

Pelejero, C., Grimalt, J.O., Heilig, S., Kienast, M., Wang, L., 1999b. High resolution U^k_{37} temperature reconstructions in the South China Sea over the past 220 kyr. Paleoceanography 14, 224–231.

Peterson, L.C., Prell, W.L., 1985. Carbonate preservation and rates of climate change: an 800 kyr record from the Indian

Ocean. The Carbon Cycle and Atmospheric CO_2 Natural Variation Archean to Present. Geophys. Monogr. 32, 251–335.

Pflaumann, U., Duprat, J., Pujol, C., Labeyrie, L.D., 1996. SIMMAX: a modern analog technique to deduce Atlantic sea surface temperatures from planktonic foraminifera in deep-sea sediments. Paleoceanography 11, 15–35.

Pflaumann, U., Jian, Z., 1999. Modern distribution patterns of planktonic foraminifera in the South China Sea and Western Pacific: a new transfer technique to estimate regional sea-surface temperatures. Mar. Geol. 156, 41–83.

Pisias, N.G., Rea, D.K., 1988. Late Pleistocene paleoclimatology of the central equatorial Pacific: sea surface response to the Southeast trade winds. Paleoceanography 3, 21–37.

Prell, W.L., 1985. The stability of low-latitude sea-surface temperature: an evaluation of the CLIMAP reconstruction with emphasis on positive SST anomalies. United States Department of Energy, Office of Energy Research, TR025, U.S. Government Printing Office 1–2, 1–60.

San Diego-McGlone, M.L., Jacinto, G.S., Dupra, V.C., Narcise, I.S., Padayao, D.O., Velasquez, I.B., 1999. A comparison of nutrient characteristics and primary productivity in the Sulu Sea and South China Sea. Acta Oceanogr. Taiwan. 37, 219–229.

Sarnthein, M., Winn, K., Duplessy, J.-C., Fontugne, M.R., 1988. Global variations of surface ocean productivity in low and mid latitudes: Influence on CO2 reservoirs of the deep ocean and atmosphere during the last 21,000 years. Paleoceanography 3, 361–399.

Schneider, R., Bard, E., Mix, A.C., 2000. Last ice age global ocean and land surface temperatures: the EPILOG initative. Pages Newsl. 8, 19–21.

Schonfeld, J., Kudrass, H.-R., 1993. Hemipelagic sediment accumulation rates in the South China Sea related to late Quaternary sea-level changes. Quat. Res. 40, 368–379.

Shaw, P.-T., Chao, S.-Y., 1994. Surface circulation in the South China Sea. Deep-Sea Res. I 41, 1663–1683.

Shaw, P.-T., Chao, S.-Y., Liu, K.-K., Pai, S.-C., Liu, C.-T., 1996. Winter upwelling off Luzon in the northeastern South China Sea. J. Geophys. Res. 101, 16435–16448.

Simmons, G.R., 1990. Subsidence history of basement sites and sites along a carbonate dissolution profile. Leg 115. Proc. ODP 115, 123–126.

Sykes, T.J.S., Ramsay, R.A.M., 1995. Calculation of mass accumulation rates in the absence of density or porosity measurements. Mar. Geol. 122, 173–179.

Szeremeta, N., Bassinot, F., Kissel, C., Bault, Y., Guibert, K., Dubois, F., Laj, C., Pagel, M., 2000. Stretching of sedimentary series collected through piston coring: evidences, implications and corrections. EOS Trans. Am. Geophys. Union 81, F708.

Thompson, P.R., Be', A.W.H., Duplessy, J.-C., 1979. Disappearance of pink-pigmented *Globigerinoides ruber* at 120,000 yr B.P. in the Indian and Pacific Oceans. Nature 280, 554–558.

Thompson, P.R., 1981. Planktonic foraminifera in the western north Pacific during the past 150,000 years: comparison of modern and fossil assemblages. Palaeogeogr. Palaeoclimatol. Palaeoecol. 35, 241–279.

Thunell, R.C., Miao, Q., Calvert, S.E., Pedersen, T.F., 1992. Glacial-Holocene biogenic sedimentation patterns in the South China Sea: productivity variations and surface water pCO_2. Paleoceanography 7, 143–162.

Wang, L., Wang, P., 1990. Late Quaternary paleoceanography of the South China Sea: Glacial–interglacial contrasts in an enclosed basin. Paleoceanography 5, 77–90.

Wang, L., Sarnthein, M., Erlenkeuser, H., Grimalt, J.O., Grootes, P.M., Heilig, S., Ivanova, E., Kienast, M., Pelejero, C., Pflaumann, U., 1999a. East Asia monsoon climate during the late Pleistocene: high-resolution sediment records from the South China Sea. Mar. Geol. 156, 245–284.

Wang, L., Sarnthein, M., Grootes, P.M., Erlenkeuser, H., 1999b. Millennial reoccurrence of century-scale abrupt events of East Asian monsoon: a possible heat conveyor for the global deglaciation. Paleoceanography 14, 725–731.

Wang, P., Wang, L., Bian, Y., Jian, Z., 1995. Late Quaternary paleoceanography of the South China Sea: surface circulation and carbonate cycles. Mar. Geol. 127, 145–165.

Wiesner, M.G., Zheng, L., Wong, H.-K., Wang, Y., Chen, W., 1996. Fluxes of particulate matter in the South China Sea. In: Ittekkot, V. et al. (Eds.), Particle Flux in the Ocean, John Wiley and Sons, pp. 293–312.

Yu, P.-S., 2000. Late Quaternary Paleoceanography and Paleoclimatology of the 'Warm Pool' South China Sea (in Chinese). M.S. Degree Thesis. National Taiwan Ocean University, 155 pp.